

# Irradiation effects in high-density polyethylene

Jussi Polvi<sup>a</sup>, Kai Nordlund<sup>a</sup>

<sup>a</sup>*Department of Physics, P. O. Box 43, FIN-00014 University of Helsinki, Finland*

---

## Abstract

Using molecular dynamics simulations, we have studied the irradiation effects in high density polyethylene. We determined the threshold energy for creating defects in the polyethylene lattice as a function of the incident angle. We found that the governing reactions were chain scissioning and generation of free radicals, whereas cross-linking and recombination of chain fragments was rare. Our analysis on the damage threshold energy shows that it's strongly dependent on the initial recoil direction and on average two times higher for the carbon atoms than for the hydrogen atoms in the polyethylene chain.

**Keywords:** molecular dynamics, irradiation, damage threshold energy, chain scission

---

## 1. Introduction

Polymeric materials such as plastics and rubber are subject to irradiation in nature due to ultra-violet light from the sun, and this is in fact a common reason for degradation of their properties. Irradiation has also been deliberately used to process and modify polymeric materials since the 1960s [1]. The earliest applications were cross-linking plastic materials, sterilizing medical equipment and preserving food products. Since then, many more practical applications for radiation processed materials have been developed and studied. For instance, electron beam cross-linking of synthetic polymers like polyethylene can be used to produce heat-shrinkable-plastic films for packaging foods, or plastic foams and hydrogels for medical applications [2, 3].

The main reactions initiated in polymers by irradiation are polymerizing (curing), grafting, chain scissioning and cross-linking. From the applications point of view, cross-linking is the most important irradiation effect in polymers. This is because it can improve the mechanical and thermal properties of the polymer, thus increasing the overall chemical, environmental and radiation stabilities of the material.

The basic idea of radiation cross-linking is simple: break chains to produce smaller fragments, for example hydrogen deficient radicals, which act as cross linking agents. Although radiation-induced cross-linking has been utilized in industry in a wide range of applications, some fundamental questions remain still open.

---

*Email address:* [jussi.polvi@helsinki.fi](mailto:jussi.polvi@helsinki.fi) (Jussi Polvi)

These questions are related to, e.g., how radicals are created near each other to induce cross-linking and how morphology influences the cross-linking reactions [4, 5].

The most often used types of irradiation for inducing cross-linking are electrons, neutrons,  $\alpha$ - and  $\beta$ -particles with kinetic energies ranging from 100 keV to 10 MeV. Also high energy gamma- and X-rays are used with photon energies from 120 keV to 10 MeV (gamma) and 100 eV to 120 keV (X-ray). Typical dose requirements for cross-linking are in the range of 50-200 kGy [3].

In order to get insight into the atomistic mechanisms of cross-linking, in this article we examine irradiation-induced defects in high density polyethylene (HDPE), using molecular dynamics (MD) simulations. Polyethylene is structurally and conceptually the simplest of the organic polymers, and experimentally HDPE has been observed to have a high tendency for cross-linking [6, 7].

A considerable number of experimental studies relating to radiation chemistry and physics of polyethylene [8, 9, 10, 11, 12] has been published, but only a few computational studies are available [13]. In a recent article by us [14] the formation of radiation defects in HDPE and cellulose was studied using MD simulations. In this work we expand and improve the previous analysis regarding irradiation effects in HDPE.

## 2. Methods

Irradiation effects in HDPE were studied using molecular dynamics simulations [15]. The simulations were carried out with the PARCAS code [16]. The inter-atomic interactions were modeled with the reactive hydrocarbon potential AIREBO [17, 18], which is based on the reactive potential model REBO, developed by Brenner [19]. This revised potential contains improved analytic functions and an extended database relative to the earlier version. These changes lead to a significantly better description of bond energies, lengths, and force constants for hydrocarbon molecules. The same potential was used by us to model HDPE in Ref. [14].

The irradiation process in the HDPE bulk was modeled by giving an initial kinetic energy, the recoil energy, to some randomly chosen atom (recoil atom) in the lattice. The direction of each collision, i.e. the direction of the initial velocity, was also generated randomly. This approach is suitable when one is not interested in sputtering or damage occurring at the surface, and when the concentration of ions in the specimen is small enough not to have a notable effect on the chemistry of the material.

Three types of simulations were carried in this work: *damage threshold simulations*, *single impact simulations* and *cumulative bombardment simulations*.

First we studied the threshold for damage production in HDPE by giving the target atom, either C or H, a recoil energy in a random direction. Using a binary search algorithm, we tuned the energy until we had pinpointed the threshold energy for creating damage in the sample by 0.5 eV precision. Due the structural simplicity of polyethylene, it is necessary to study only one carbon and one hydrogen atom to get

a description of all the atoms in the system.

The definition for 'damage', used in our damage threshold simulations, is that at least one bond in the target sample is broken as a consequence of the recoil event. This means that the target atom and its bonds may be unaffected if the broken bond is a secondary effect. The simulation time used in these simulations was 3 ps.

In the single impact simulations, 100 simulations were carried out per recoil energies 5, 10, 20, 50 and 100 eV. Each simulation was run for 10 ps to give the system some time to relax after the initial recoil, and for all interesting reactions time to happen. In 50 simulations a random hydrogen atom was chosen as a recoil atom, and in another 50 simulations, a random carbon atom. The single impact simulation process identical to the one used in in Ref. [14], but we get the larger statistics, add H recoils and we analyze the results differently.

To model a real-life application of irradiation, transmission electron microscope (TEM) imaging, we produced recoil energies corresponding to 200 and 500 keV electron irradiation, and consecutively bombarded the HDPE sample with 20 of such recoil events. For each event, the recoiling atom was chosen to be either H or C based on the integrated threshold cross-section sections <sup>1</sup> of the atoms, and taking into account that in PE there are two hydrogen for each carbon. After the recoil atom was chosen, it was given a recoil energy selected randomly according to the distribution shown in Fig. 7.

We carried out 20 sets of cumulative bombardment simulations for both 200 and 500 keV electron energies. In these simulations, the simulation time was from 3 to 10 ps depending on the recoil atom type and energy. Between each recoil event, the system was relaxed and cooled down with the Berendsen temperature control [21] applied to all atoms and including Berendsen pressure control [21], with a time constant of 200 fs.

In all simulations an orthorhombic high density ( $\rho = 0.98 \text{ g/cm}^3$ ) polyethylene crystal, relaxed at 0 K, was used as the target sample. Periodic boundary conditions were used in all directions. During irradiation, temperature control was applied at the simulation cell borders (thickness 3 Å), to scale the temperature there towards 0 K.

### 3. Results

In the damage threshold simulations, the size of the simulation box was  $x=2.9 \text{ nm}$ ,  $y=2.5 \text{ nm}$  and  $z=2.6 \text{ nm}$ , containing 2400 atoms, and the polymer chains were oriented along the  $z$ -axis.

In the single impact and cumulative bombardment simulations, the size of the simulation box was  $4 \times 7 \times 16$  unit cells, with dimensions of  $x=2.9 \text{ nm}$ ,  $y=3.6 \text{ nm}$  and  $z=4.1 \text{ nm}$ . The simulation system consisted of 5376 atoms. Irradiation of this system with 10 eV of energy corresponds to a 38 kGy dose of ionizing radiation.

---

<sup>1</sup>Calculated using the McKinley & Feshback formula [20].

### 3.1. Damage threshold simulations

Fig. 1 shows the recoiling atoms for the damage threshold simulations; carbon highlighted in red, hydrogen in blue. The chains are oriented along the  $z$ -axis, and in the following energy maps, the 'up' or 'north' direction is same as 'up' in the Fig. 1.

Based on our simulations the average energy needed to create damage in the PE sample was 10.2 eV for H recoils, and 19.9 eV for C recoils. This is in good agreement with TEM experiments, according to which the electron energy needed to induce defects in polyethylene is about 100 keV [22]. This corresponds to a maximal energy transfer of 20 eV to a carbon atom. On the other hand, 100 keV electron energy also corresponds to a maximum energy transfer of 240 eV to H atoms, i.e. well above the threshold. The fact that no damage is observed in TEMs is most likely due to the fact that almost all damage produced by H recoils is H radicals or  $H_2$  molecules (see also Fig. 5). H atoms are not normally visible in TEMs and hence damage involving H is not observable. Moreover, H radicals have a high probability to recombine with reactive carbons.

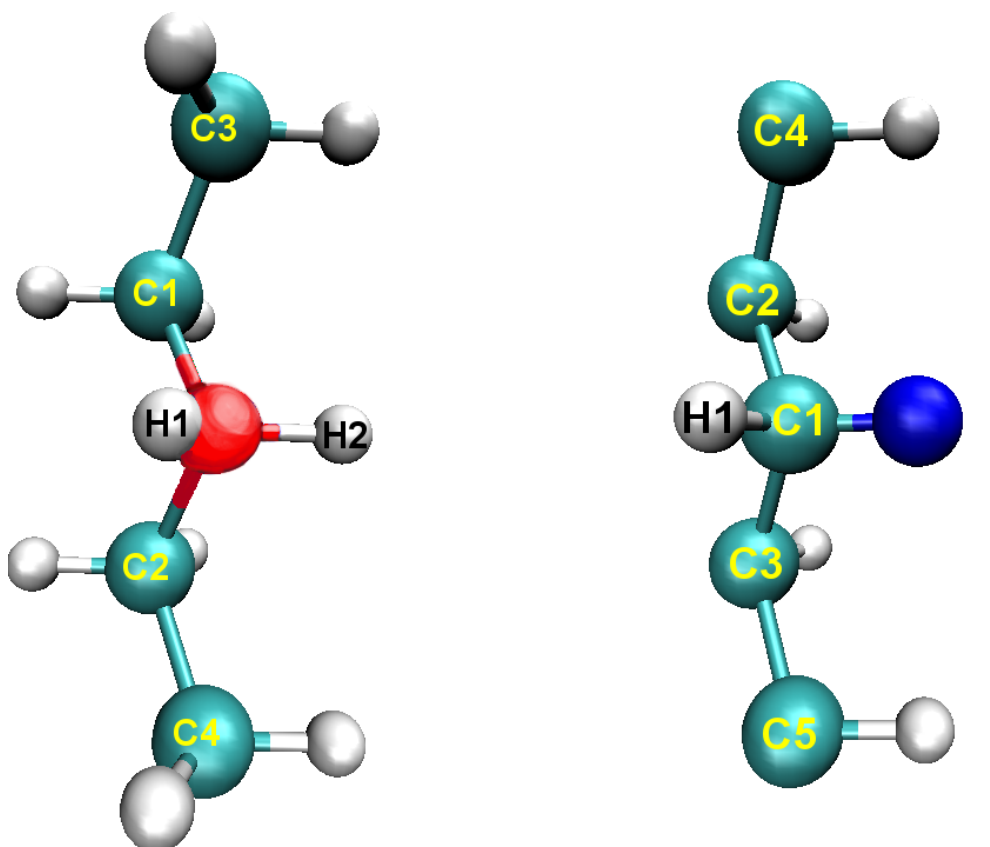


Figure 1: A visualization of the recoil atoms for damage threshold simulations. On the left is shown the recoiling carbon atom (red) and on the right the recoiling hydrogen atom (blue). The numbers drawn on the atoms correspond to the numbers on energy landscape images.

In Fig. 2 and Fig. 3 we have the energy landscapes of the damage threshold energy for a carbon atom and a hydrogen atom in polyethylene chain. Both damage threshold energy maps are based on 500 recoil events with a random initial recoil direction. Note that as spherical maps stretched to planar maps, the polar regions in the images are strongly elongated in the horizontal direction. Using these 500 data points as base values, the map grid is filled with interpolated values, of which the final map is composed. The white bands in the top and bottom of the maps are caused by insufficient number of data points occurring in the pole regions due their small area.

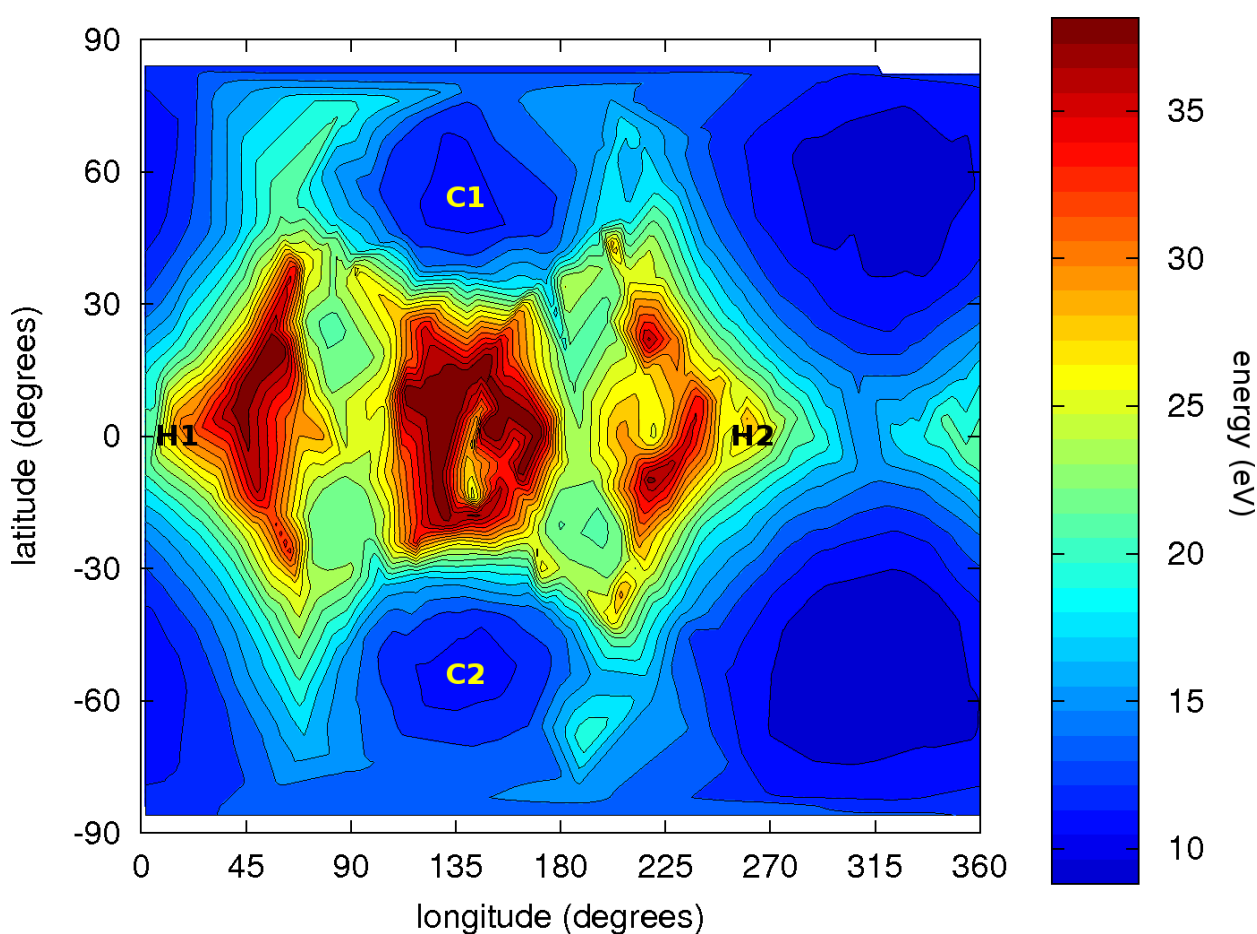


Figure 2: A 2D energy landscape showing the damage threshold energy of a carbon atom in PE chain, as a function of spherical coordinates, latitude on the  $y$ -axis and longitude on the  $x$ -axis.

In Fig. 2, the damage threshold map for carbon atom in PE, we see threshold energy values ranging from 8.8 eV to 40 eV. Creating damage requires most energy (red regions in the map) when the recoil pushes the target carbon atom between its carbon neighbors, or perpendicular to that direction in equatorial zone of the map.

Damage is created with the lowest recoil energies when the carbon atom is pushed along the direction of

its C-C bonds. In these cases, most of the recoil energy is used for breaking a single C-C bond, instead of dividing it more evenly between two C-C bonds. Generally damage is more easily created by recoils along the chain direction (towards poles) than by recoils perpendicular to the chain direction. Also in about 10% of the cases the recoil event leaves C-C bonds intact but causes the recoiling carbon to shake off one of its hydrogen neighbors.

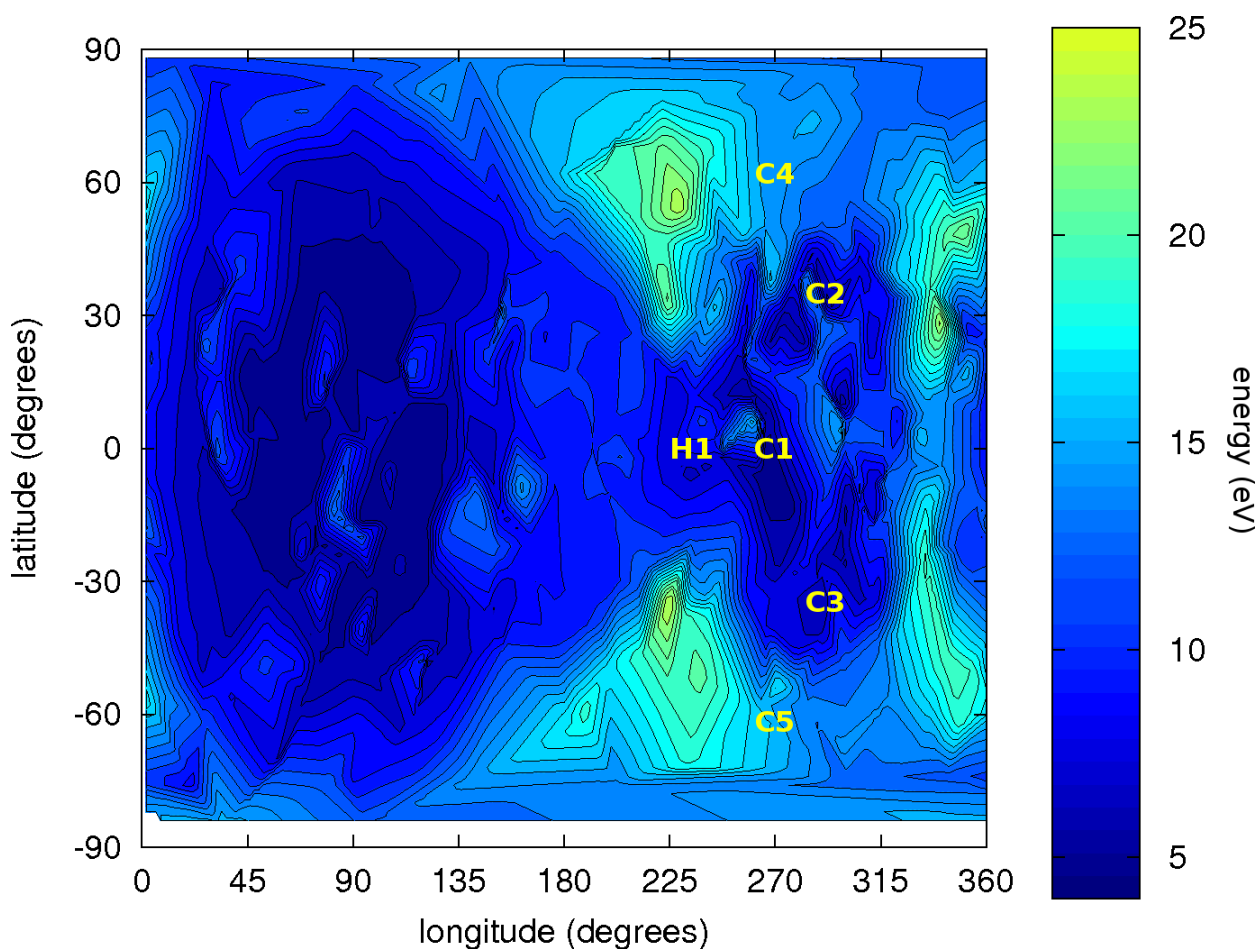


Figure 3: A 2D energy landscape showing the damage threshold energy of a hydrogen atom in PE chain, as a function of spherical coordinates, latitude on the  $y$ -axis and longitude on the  $x$ -axis.

The damage threshold map for hydrogen atom in PE is shown in Fig. 3. The color scale is set to match the one used in Fig. 2, so one immediately notices that on average, the threshold energy for creating damage by hydrogen recoils is considerably lower than the threshold energy for carbon. The lowest threshold energies are 4.5 eV and the highest 25 eV.

Damage is created with lowest energies when the hydrogen atom is pushed away from its chain (the large blue region on the left-hand side of Fig. 3). Similar but smaller low threshold region can also be seen in the direction of the nearest carbon atoms (C1, C2 and C3). When damage is created it typically means that

the recoiling hydrogen breaks its H-C bond. In about 4% of the cases the damage is caused by the neighbor hydrogen (H1 in the Fig. 1) breaking free from C1, and in about 2% of the cases the first damage to occur is the breaking of the PE chain.

In those events where the threshold energy is largest, the recoil energy appears to be transferring from the recoiling hydrogen to the polymer chain, bending and twisting the chain, and in many cases the chain breaks momentarily but then the dangling bonds immediately recombine.

### 3.2. Single impact simulations

Table 1 shows the statistics of the different kinds of damage caused by the single impact simulations at recoil energies between 5 and 100 eV. With each energy, 50 hydrogen recoils and 50 carbon recoils were simulated.

With the recoil energy of 5 eV, no bond breaking occurred with either of the recoil types. With 10 eV H recoils, free molecules (hydrogen radicals) were observed in 42% of the cases. 10 eV C recoils gave broken PE-chains (chain scission) in 10% of simulations, but no free molecules as the recoil atom always remained covalently bound to its initial chain. These results are consistent with expectations from the damage threshold simulations.

At 20 eV, broken chains were observed after 10% of H recoils and 48% of C recoils. Free molecules were produced only after H recoils; hydrogen radicals in 64%, and molecular hydrogen in 4% of the cases. With recoil energies 30 and 50 eV, broken chains and free molecules are formed after both H and C recoils. Broken chains are the more common type of damage after C recoils, and free molecules are more common as a result of H recoils. The free molecules produced by H recoils are again all either H atoms or H<sub>2</sub> molecules, but C recoils produce also some hydrocarbon radicals.

For the 100 eV recoils, both recoil atom types produce more free molecules than broken chains. After H recoils, we observed  $0.64 \pm 0.11$  broken chains per recoil event, and chain scission was observed in 42 % of the simulation system, and in about half of the cases two chains were broken. In C recoil simulations, chain scission was observed after all recoil events, and two broken chains were observed in half of the cases. Cross-links were also observed in 4% (two cases of 50) of the C recoils simulations.

The average recoil atom path lengths in the single impact simulations are plotted in the Fig. 4. (The average length is calculated only from those recoil atoms that break free from the original chain.) 46% of the hydrogen recoil atoms are broken free from their C-H bonds already at 10 eV recoil energy, and at 30 eV 90% of them. Carbon recoil atoms are connected to their original chains with two C-C bonds and are thus harder to dislodge. At recoil energies of 20 eV and less, all carbon recoils still have at least one C-C bond with the original chain. At 30 eV, 18% of the C recoil atoms are broken free; at 50 eV, 42%; and at 100 eV, 88% of the recoil atoms break both of their C-C bonds. The distances traveled by hydrogen recoil atoms

Table 1: Broken chains, free molecules and cross-links formed in HDPE during single impact simulations.

recoil energy [eV]	recoil atom	broken chains	free molecules	cross-links
<b>5</b>	H	0.0	0.0	0.0
	C	0.0	0.0	0.0
<b>10</b>	H	0.0	0.42±.09	0.0
	C	0.10±.04	0.0	0.0
<b>20</b>	H	0.10±.04	0.68±.12	0.0
	C	0.48±.10	0.0	0.0
<b>30</b>	H	0.14±.05	0.94±.14	0.0
	C	0.86±.13	0.22±.07	0.0
<b>50</b>	H	0.24±.07	1.5±.2	0.0
	C	1.0±.1	0.58±.11	0.0
<b>100</b>	H	0.64±.11	2.4±.2	0.0
	C	1.5±.2	2.4±.2	0.04±.03

are about twice as long as the distances traveled by carbon recoils. Even with 100 eV recoil energy, the recoiling carbon atom usually moves no farther than the nearest neighbor chain, at 4.1 Å distance.

We also tested calculating the recoil atom path lengths with the widely used binary-collision approximation code SRIM [23, 24]. We ran SRIM simulations of H and C implantation into a random C-2 H-4 atom mixture. SRIM does not have any information on atomic structure as the atom position are obtained by a Monte Carlo algorithm determining the impact parameter of the next collision [25, 23]. The SRIM input parameters on displacement energy and lattice binding energy were obtained from the standard "Compound dictionary" of the software, but the density was changed to the same value (0.98 g/cm<sup>3</sup>) as in the MD simulation. We obtained mean ranges of 47 Å and 14 Å for 100 eV and 20 eV H ions, and 16 Å and 8 Å for 100 eV and 20 eV C, respectively. Comparison with the results in Fig. 4 shows that the SRIM ranges are roughly a factor of 3 higher than the MD results. This comparison shows that the ion movement is strongly affected by the structure and chemical bonding in polyethylene, and that the binary collision approximation is (at least without major recalibration of the parameters) not suitable for simulation of recoils in organic materials at energies  $\lesssim$  100 eV.

The distribution of free radicals and other molecules in 50 and 100 eV simulations is shown in Fig. 5. The most abundant radical types are H and CH<sub>x</sub>, but some non-reactive H<sub>2</sub> molecules were also produced, especially by H recoils. The 100 eV recoils produced about 2.5 times more free radicals and molecules than the 50 eV recoils, namely 4.8±.2 versus 2.1±.1 radicals per recoil. The C recoils produce a wider distribution

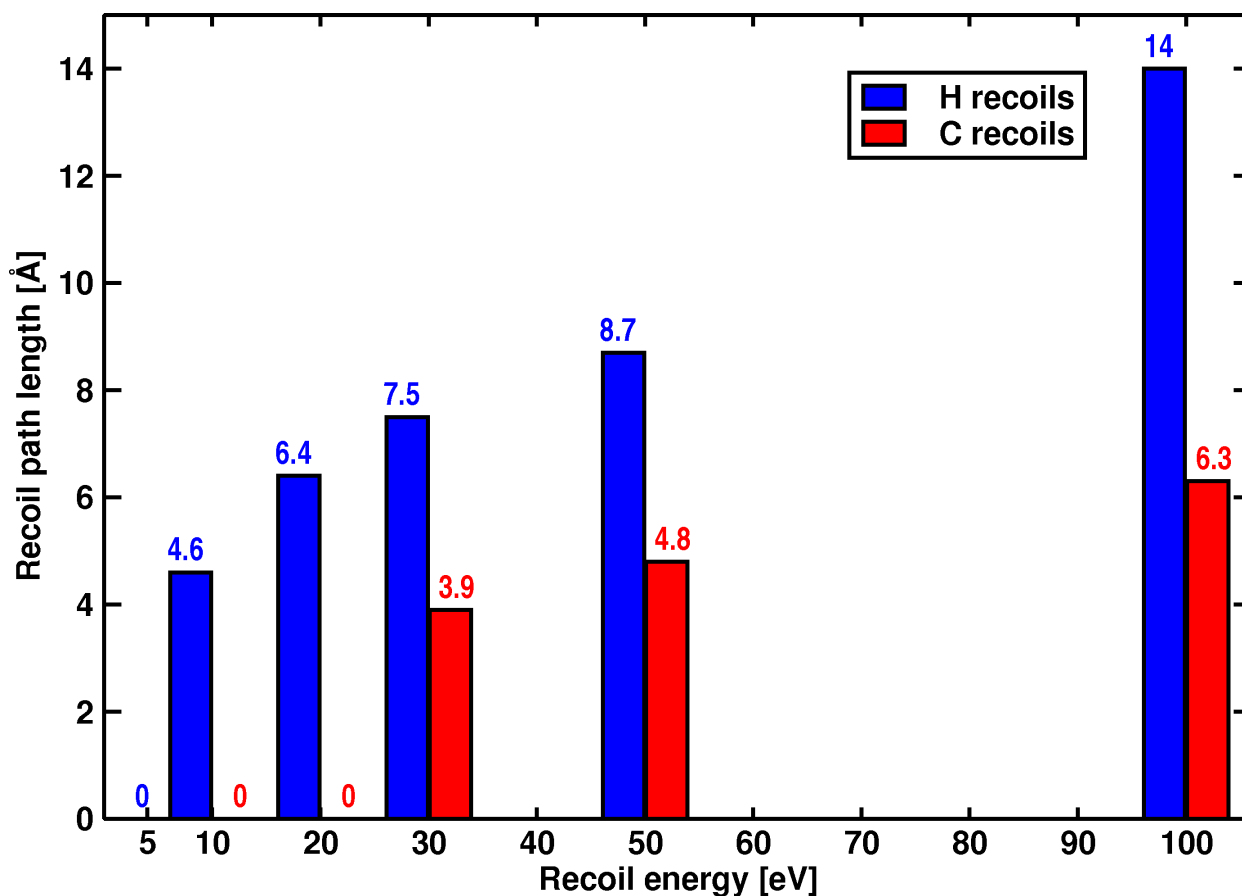


Figure 4: Recoil atom path lengths from single-impact simulations. Blue bars are for hydrogen recoil atoms, red bars for carbon.

of different molecules, while H recoils create mostly H and H<sub>2</sub>.

In Fig. 6 we have the mass distribution of the molecules created in the single impact simulations. The mass of the free molecules, for both C and H recoils, increases linearly. This differs from the case of the number of free molecules: as we can see from the Table 1, the number of free molecules created by H recoils increases sublinearly as a function of energy, and the number of free molecules created by C recoils increases superlinearly.

The slope of the mass increase for C recoils is about 5 times steeper than for the slope for H recoils. This is explained by the fact that the heavier C recoil atom is much more efficient than hydrogen in breaking C-C bonds and creating heavier radicals.

### 3.3. Cumulative bombardment

In the cumulative bombardment simulations, we modeled the effect of electron irradiation such as TEM imaging, using electron energies 200 and 500 keV. A typical TEM voltage for studying organic materials

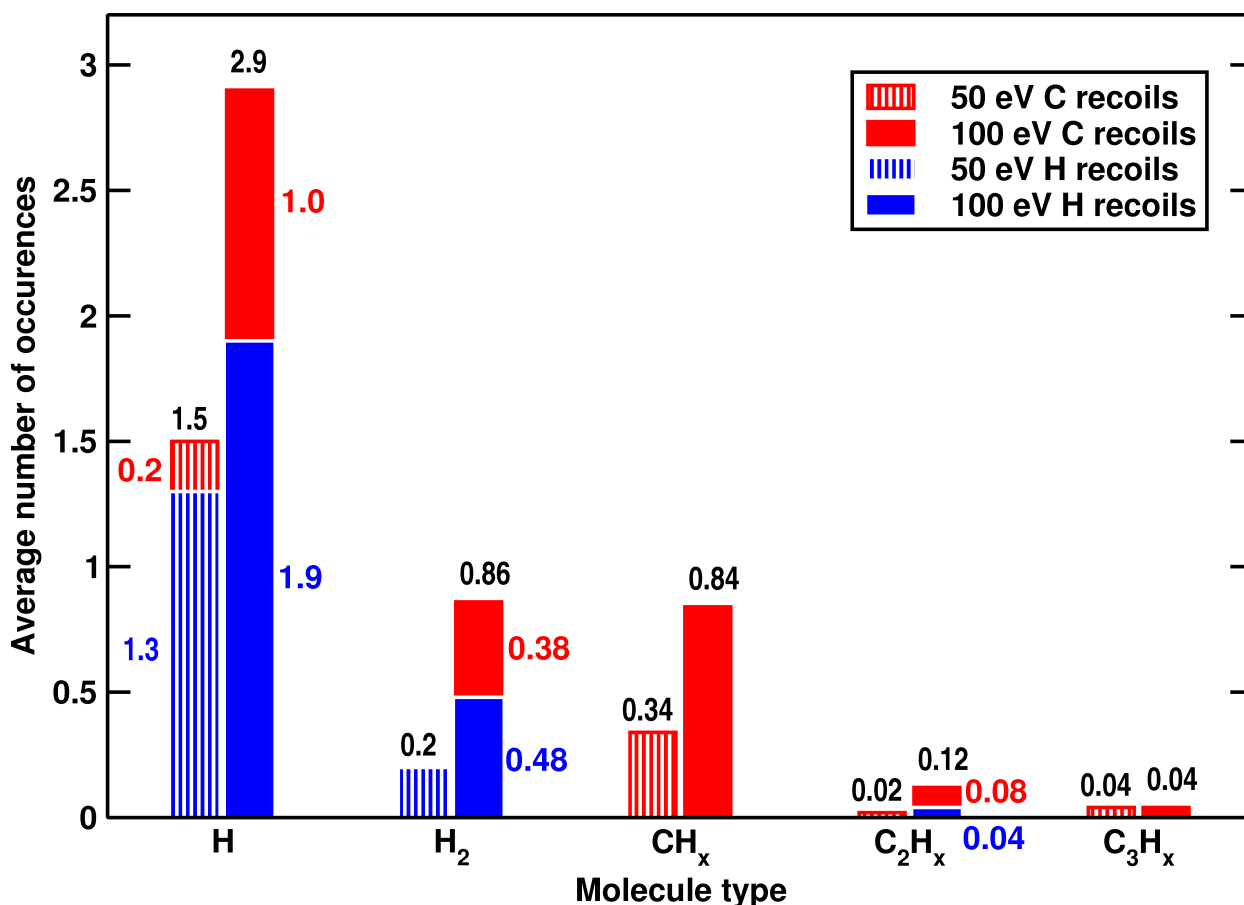


Figure 5: Distribution of different types of free molecules created during single impact simulations. Blue bars correspond to the number of molecules created by 50 (striped) and 100 eV (full color) H recoils; red bars show the number of additional molecules created by C recoils.

such as polyethylene is 100 keV [22, 26], but based on our single impact simulation results it is clear that 100 keV electrons would produce so little damage in our simulations that we deemed it to be more fruitful to model electron irradiation with slightly higher energies.

In the 200 keV simulations, the recoil atom was C with 23% probability and H with 77% probability. In 500 keV simulations the probabilities were 33% and 67%, respectively. The recoil energy for each event was chosen randomly according to the energy distributions shown in Fig. 7.

The lowest recoil energies used for H and C, 10 and 20 eV, are based on the average displacement energies for H and C, calculated from the damage threshold simulation results.

Table 2 shows broken chains, free molecules and cross-links created during the cumulative bombardment. Both 200 and 500 keV simulation sets included 20 simulation systems with 20 cumulative recoil events for each system, 400 recoil events in total for both electron energies. In 200 keV simulations, the average recoil energy was 31.4 eV (32.7 eV for H recoils and 27.7 eV for C recoils) and in 500 keV simulations it was

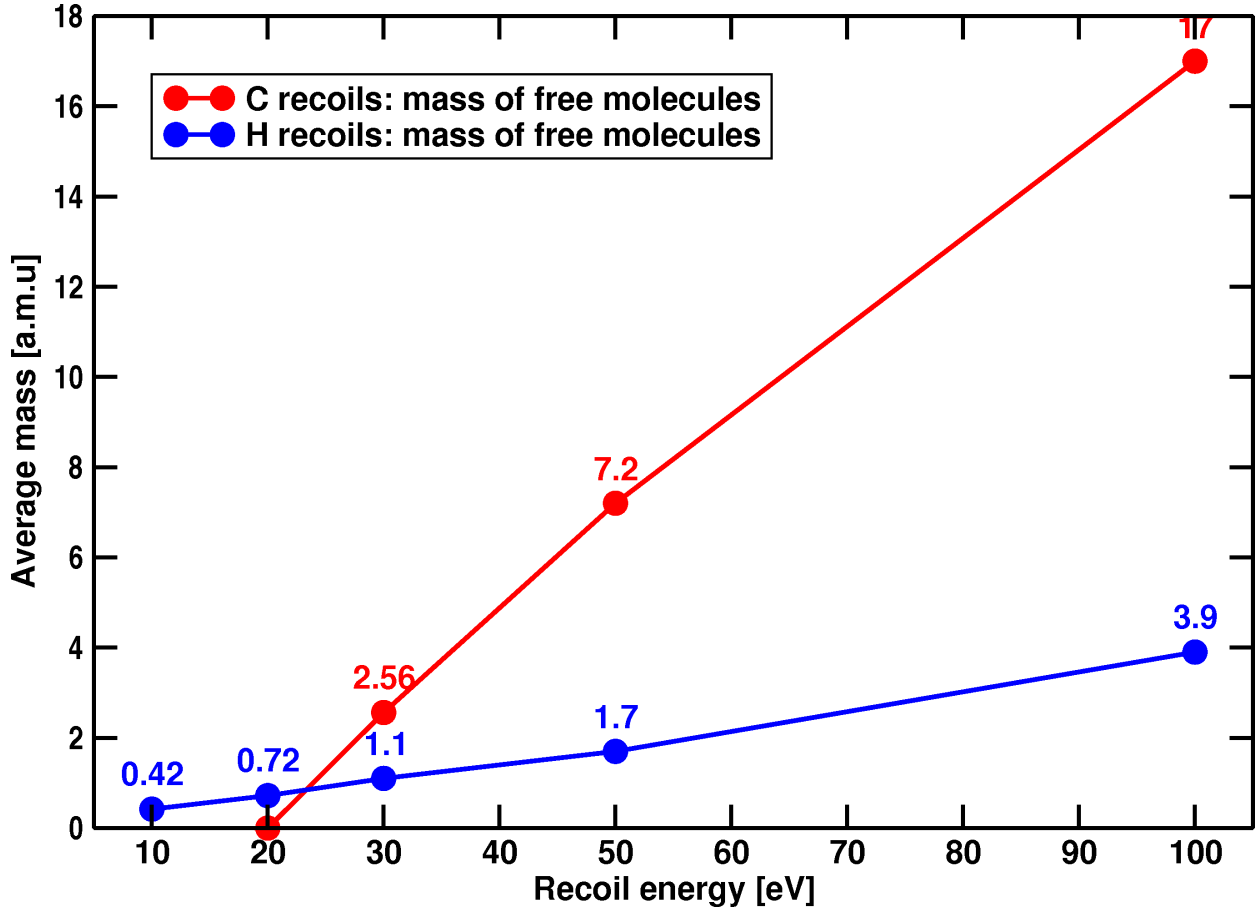


Figure 6: Mass distribution of free molecules as a function recoil atom energy. Blue line the mass of molecules created by H recoils; red line the mass of molecules created by C recoils.

43.5 eV (46.0 eV for H recoils and 38.1 eV for C recoils). We can see that even though the electron energy in the latter case is 2.5 times larger, the average recoil energy is increased by less than 40%. Due the shape of the energy distribution, the median recoil energy values are considerably less than the averages; 17 and 18 eV for 200 and 500 keV H recoils, and 26 and 30 eV for C recoils. No cross-links were produced in the cumulative bombardment simulations.

The numbers for broken chains and free molecules in table 2 correspond to damage produced by 20 recoil events. Thus a single 200 keV electron collision causes  $0.08 \pm 0.01$  broken chains and  $0.28 \pm 0.03$  free molecules on average to the target sample. For 500 keV electrons these numbers are  $0.13 \pm 0.02$  and  $0.31 \pm 0.03$ , respectively. Comparing these numbers to the single impact simulations, we see that the damage caused by these events is less than what we observed after single impact simulations with similar recoil energies. The reason for this is that the recoil energy distribution used here (shown in Fig. 7) is peaked at lowest recoil energies and thus majority of the recoil events have such low energies that producing damage is unlikely.

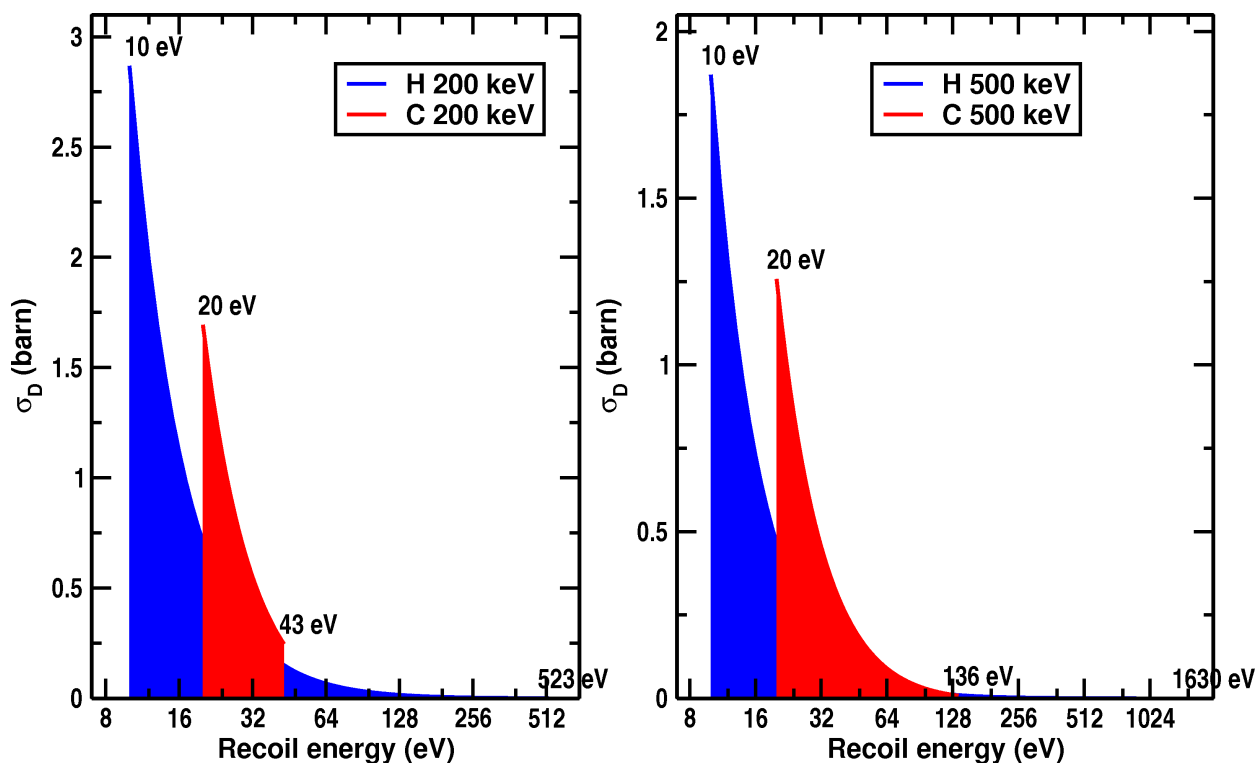


Figure 7: Threshold cross-section of carbon (red) and hydrogen (blue) as a function of recoil energy for 200 keV (left plot) and 500 keV (right plot) electron irradiation. The recoil energies used in the cumulative bombardment simulations were produced with these distributions.

Figure 8 shows the average distribution of free molecules after 20 consecutive impacts with recoil energies corresponding to 200 keV and 500 keV electron irradiation. After 200 keV electron bombardment (green bars in the figure) most of the free molecules in the system are hydrogen radicals H, with 20% of H<sub>2</sub> and 7% CH<sub>x</sub> radicals. 500 keV electron bombardment (violet bars) create a wider distribution of free molecules; hydrogen radicals are still most abundant but now we have 34% of H<sub>2</sub> and 18% of various hydrocarbon radicals. This is to be expected since the recoil atoms are mostly hydrogens and from single impact results (Fig 5) we see that H recoils produce mostly H and H<sub>2</sub>.

### 3.4. Discussion

We found that the occurrence probability for cross-linking in HDPE to be small. Only in 100 eV single impact simulations, we observed  $0.04 \pm 0.03$  cross-links per carbon recoil event and no cross-links in cumulative bombardment simulations.

The threshold displacement energy for carbon is well in line with the TEM experimental threshold. The simulated H threshold energy is much lower than the maximum energy transfer for 100 keV electrons, which indicates that, even though H atoms may be displaced in typical TEM imaging conditions, they have a high

Table 2: Broken chains, free molecules and cross-links formed in HDPE during cumulative bombardment simulations

electron energy [keV]	ave. recoil energy [eV]	broken chains	free molecules	cross- links
<b>200</b>	31.4	1.55±.28	5.55±.53	0
<b>500</b>	43.5	2.55±.35	7.10±.55	0

propensity to recombine with dangling bonds in the C chains, and hence do not lead to observable damage.

Finally, it is important to note that these simulations do not give a complete picture of the irradiation effects in polyethylene for all kinds of irradiation. For many kinds of irradiation, electronic effects may excite bonds into antibonding states and hence also cause bond breaking. The current results should describe well the atomic collision part of the damage production, which also includes the damage from impact transfer from high-energy electrons to atomic nuclei [20].

#### 4. Conclusions

The irradiation effects on HDPE have been examined using atomistic simulations to better understand the reactions that occur inside the material and to obtain insight into the mechanism of cross-linking.

Our results illustrate the probability and nature of damage produced by low-energy recoils in high-density, crystalline polyethylene. The results show that the threshold energy for C strongly depends on the direction of the initial recoil with respect to the covalent bonds to the neighboring carbon atoms. The H threshold energy was found to be on average about half of the C threshold energy and somewhat less dependent on the recoil direction. Above the threshold energy, single C recoils up to 100 eV are found to produce predominantly free H atoms and H<sub>2</sub> molecules, but also a significant fraction of free hydrocarbon molecules. H recoils produce solely H and H<sub>2</sub> with recoil energies up to 50 eV, and also with 100 eV recoils the fraction of hydrocarbon radicals is only a few percent. Cross-linking was in the current simulations observed only for 100 eV C recoils, and even for these the probability was only a few percent.

#### Acknowledgments

Grants of computer time from CSC – IT Center for Science Ltd in Espoo, Finland, are gratefully acknowledged. J.P. acknowledges funding from SMARTWOOD project and from Waldemar von Frenckells stiftelse.

#### References

- [1] Gould, R. F. *Irradiation of Polymers*; American Chemical Society: Washington, D.C., USA, 1967.

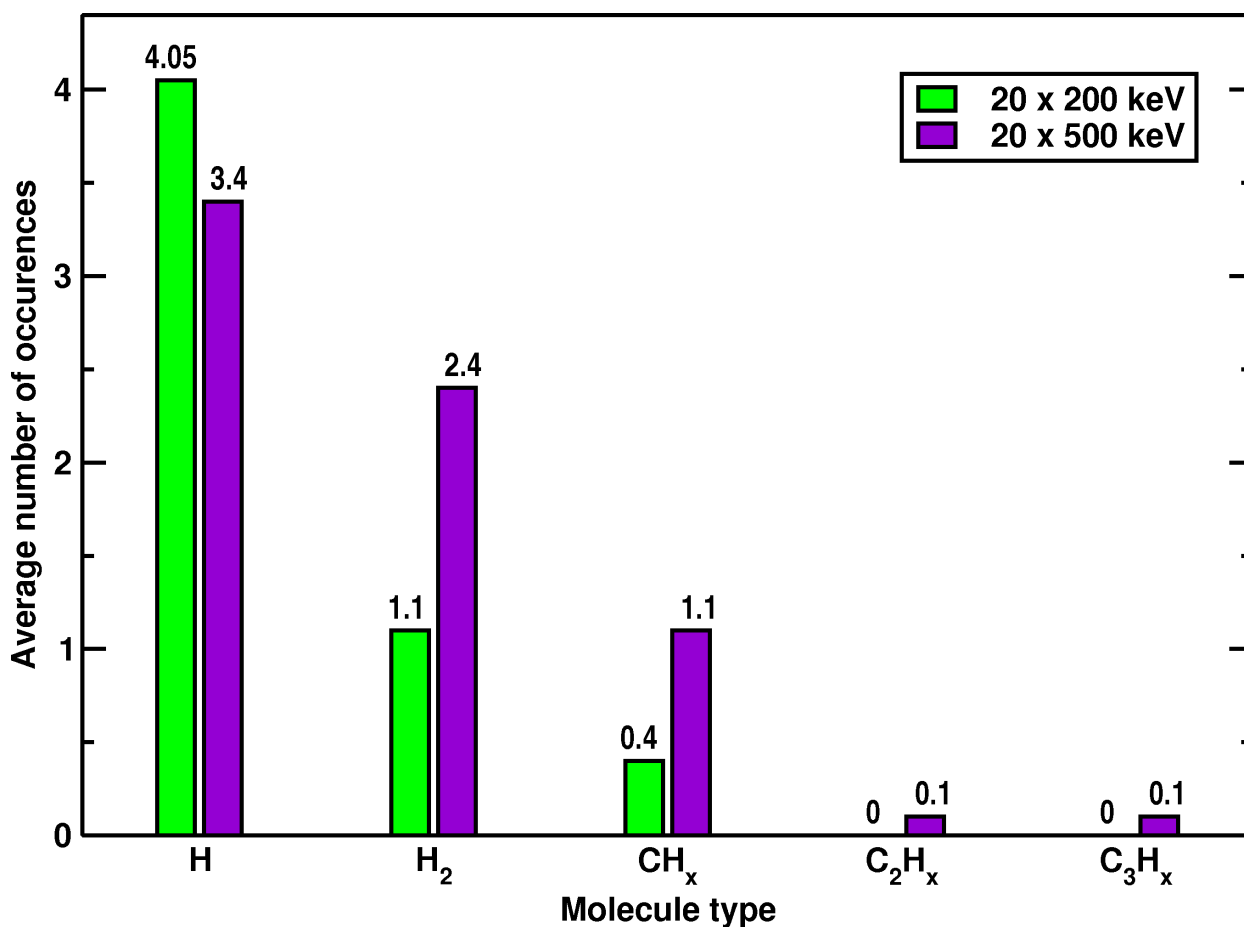


Figure 8: Average distribution of free radicals and other molecules in PE after 20 consecutive recoils with energies corresponding to 200 keV electrons (green bars) and 500 keV electrons (violet bars).

- [2] Przybytniak, G.; Nowicki, A. *NUKLEONIKA* **2008**, *53(Suppl. 2)*, s67–s72.
- [3] Cleland, M. R.; Parks, L. A.; Cheng, S. *Nucl. Instr. Meth. Phys. Res. B* **2003**, *208*, 66–73.
- [4] Gehring, J.; Zybball, A. *Radiat. Phys. Chem.* **1995**, *46*, 931–936.
- [5] Patel, G. N.; Keller, A. *J Polym Sci: Polym Phys* **1975**, *13*, 303–321.
- [6] Driscoll, M. *Radiation Physics and Chemistry* **2009**, *78*, 539–542.
- [7] Kovalev, G. V.; Bugaenko, L. T. *High Energy Chemistry* **2003**, *37*, 209–215.
- [8] Charlesby, A. *Atomic radiation and polymers*; Pergamon Press Inc., 1960.
- [9] Chapiro, A. *Radiation Research Supplement* **1964**, *4*, 179–191.
- [10] Singh, A. *Radiation Physics and Chemistry* **1999**, *56*, 7556–7570.
- [11] Thomas, J. K. *Nucl. Instr. and Meth. B* **2007**, *265*, 1–7.
- [12] Perez, C. J. *Radiation Physics and Chemistry* **2010**, *79*, 710–717.
- [13] Beardmore, K. *Nuclear Instruments and Methods in Physics Research B* **1995**, *102*, 223–227.
- [14] Polvi, J.; Luukkonen, P.; Järvi, T. T.; Kemper, T. W.; Sinnott, S. B.; Nordlund, K. *J. Phys. Chem. B* **2012**, *116*, 13932–13938.
- [15] Allen, M. P.; Tildesley, D. J. *Computer Simulation of Liquids*; Oxford University Press: Oxford, England, 1989.

- [16] Nordlund, K. 2006, PARCAS computer code. The main principles of the molecular dynamics algorithms are presented in [? ]. The adaptive time step and electronic stopping algorithms are the same as in [? ].
- [17] Stuart, S. J. *Journal Of Chemical Physics* **2000**, *112*, 6472–6486.
- [18] Brenner, D. W.; Shenderova, O. A.; Harrison, J. A.; Stewart, S. J.; Ni, B.; Sinnott, S. B. *Journal of Physics: Condensed Matter* **2002**, *14*, 783–802.
- [19] Brenner, D. W. *Physical Review B* **1990**, *42*, 9459–9471.
- [20] McKinley, W.; Feshbach, H. *Phys. Rev.* **1948**, *74*, 1759–1763.
- [21] Berendsen, H. J. C.; Postma, J. P. M.; van Gunsteren, W. F.; DiNola, A.; Haak, J. R. *J. Chem. Phys.* **1984**, *81*, 3684–3690.
- [22] Egerton, R. F.; Li, P.; Malac, M. *Micron* **2004**, *35*, 399–409.
- [23] Ziegler, J. F.; Biersack, J. P.; Ziegler, M. D. *SRIM - The Stopping and Range of Ions in Matter*; SRIM Co.: Chester, Maryland, USA, 2008.
- [24] Ziegler, J. F. SRIM-2008.04 software package, available online at <http://www.srim.org>.
- [25] Ziegler, J. F.; Biersack, J. P.; Littmark, U. *The Stopping and Range of Ions in Matter*; Pergamon: New York, 1985.
- [26] Zhou, H.; Wilkes, G. *Polymer* **1997**, *38*, 5735 – 5747.